Journal of Catalysis **191,** 423–429 (2000)
doi:10.1006/jcat.2000.2810, available online at http://www.idealibrary.com on IDEAL®

Synthesis and Decomposition of Formate on a Cu/SiO_2 Catalyst: Comparison to Cu(111)

T. Yatsu,* H. Nishimura,* T. Fujitani,† and J. Nakamura*,[1]

*Institute of Materials Science, University of Tsukuba, Tsukuba, Ibaraki 305-8573, Japan; and †National Institute for Resources and Environment, Tsukuba, Ibaraki 305-8569, Japan

Received September 22, 1999; revised December 27, 1999; accepted January 4, 2000

The kinetics of formate synthesis from CO_2 and H_2 and from formate decomposition on Cu/SiO_2 were studied by temperature-programmed decomposition experiments and compared with those reported for Cu(111), Cu(110), and Cu(100) surfaces under similar reaction conditions. The initial rate of the formate synthesis from 380 Torr CO_2/380 Torr H_2 at 323–353 K over the Cu/SiO_2 catalyst was in good agreement with those on Cu(111) and Cu(110). At 353 K, for example, the initial rate was measured to be 5.3×10^{-4} molecules site^{-1} s^{-1}. The apparent activation energy was determined to be 58.8 kJ mol^{-1}, which was also comparable with those obtained for Cu(111) (54.6–56.6 kJ mol^{-1}), Cu(110) (59.8 kJ mol^{-1}), and Cu(100) (55.6 kJ mol^{-1}). The decomposition rate of formate was first-order in formate coverage, and the rate constant was 1.13×10^{-4} s^{-1} at 384 K. The activation energy and the pre-exponential factor were determined to be 115.7 kJ mol^{-1} and 5.38×10^{11} s^{-1}, respectively, in good agreement with those obtained for Cu(111), 107.9–112.8 kJ mol^{-1} and $(1.87–4.02) \times 10^{11}$ s^{-1}, rather than those for Cu(110) (145.2 kJ mol^{-1} and 1.22×10^{16} s^{-1}) and Cu(100) (130–155.0 kJ mol^{-1}). The promotional effect of H_2 upon the decomposition of formate was observed on the Cu/SiO_2 catalyst as observed for Cu(111) but not for Cu(110). The decomposition rate of formate on Cu/SiO_2 was promoted by a factor of 6 at an H_2 pressure of 457 Torr. These kinetic results clearly indicate that the surface of Cu particles supported on SiO_2 comprises Cu(111) planes. Equilibrium formate coverage on Cu/SiO_2 during the hydrogenation of CO_2 was well reproduced by the calculated coverage based on the kinetics of the formate synthesis and the formate decomposition. However, the equilibrium formate coverage on Cu/SiO_2 was greater than that measured for Cu(111) under the same reaction conditions because the hydrogen-promoting decomposition rate on Cu/SiO_2 is less than that on Cu(111). This is explained by a decrease in hydrogen coverage on Cu surfaces of the Cu/SiO_2 catalyst caused by the spillover of hydrogen atoms from Cu onto the SiO_2 surface. Thus, the effect of SiO_2 was observed in the hydrogen-promoting decomposition kinetics on Cu.

Key Words: **formate species; copper catalyst; carbon dioxide; hydrogen.**

1. INTRODUCTION

Surface science is widely known to be very useful in investigating the mechanism of catalytic reactions on model single-crystal surfaces at the atomic level. In order to establish the model of real catalysts, the catalytic activity of single-crystal surfaces should be measured under medium- or high-pressure conditions (1–50 atm) (1, 2). Once a catalyst model is realized on a single-crystal surface, various kinds of surface science techniques are available to examine surface structure, reactivity, and electronic structure on the atomic level. One thus always has to compare the kinetics of catalytic reactions or elementary steps on model catalysts with those for real catalysts under comparable reaction conditions. In this study, we compare the kinetics of formate synthesis on a powder catalyst with those on single-crystal model catalysts under atmospheric pressure conditions.

We have studied the methanol synthesis by hydrogenation of CO_2 over Cu–Zn-based catalysts using classical methods for powder catalysts (3–7), surface science techniques (8–13), and ab initio calculation (14). As a result, we have successfully established the model of Cu/ZnO powder catalysts by depositing Zn atoms on a Cu(111) surface. The structure, the oxidation state, and the role of the active sites on the Zn/Cu(111) surface have been further studied by X-ray photoelectron spectroscopy (XPS) (8, 9, 11), *in situ* infrared reflection absorption spectroscopy (IRAS) (10, 12), and scanning tunneling microscopy (STM) (11, 13) as well as high-pressure reactors, which are reviewed elsewhere (15). We then attempted to establish the microkinetics of elementary steps constituting the methanol synthesis reaction on single-crystal surfaces as well as Cu powder catalysts. We have thus initially reported the kinetics for the synthesis of the formate intermediate by hydrogenation of CO_2 as well as the formate decomposition on Cu(111), Cu(110), and Zn/Cu(111) surfaces (12, 16, 17). In the present study, we measure the kinetics of formate synthesis and decomposition on Cu/SiO_2 and compare it with those previously reported on Cu(111) and Cu(110) surfaces.

[1] To whom correspondence should be addressed. Fax: 81-298-55-7440. E-mail: nakamura@ims.tsukuba.ac.jp.

0021-9517/00 $35.00

We have observed some of the following interesting features in the formate chemistry on Cu surfaces: (i) The decomposition of formate synthesized on Cu(111) in the presence of H_2 proceeded faster than that in ultrahigh vacuum (UHV) by an order of magnitude (18). Furthermore, the synthesis of formate on Cu(111) and Cu(110) showed a structure-insensitive feature in terms of the activation energy, whereas the decomposition of formate on Cu surfaces was structurally sensitive (12). In the STM studies, formate synthesized from CO_2 and H_2 on Cu(111) was found to adsorb linearly like molecular chains with the distance between the chains decreasing with increasing formate coverage (13). However, no chain structure was observed for the formate prepared by the adsorption of formic acid (13). (ii) The decomposition rate of the formate was greater than that of formate synthesized from CO_2 and H_2 by an order of magnitude (17, 18), which was explained by the difference in the adsorption structure of formate (13). (iii) The decomposition rate of the formate prepared from CO_2 and H_2 was promoted by the presence of H_2 (18). (iv) The promoted decomposition rate became equal to the decomposition rate of the formate prepared from formic acid. We here study whether these characteristic features appear in the Cu/SiO_2 powder catalyst (18).

The decomposition of formate on a Cu/SiO_2 catalyst (19), Cu powder (20), Cu(110) (21–24), and Cu(100) (25, 26) has been widely reported by several researchers, but the formate was prepared by the adsorption of formic acid except for in the report by Taylor *et al.* (26), who carried out the kinetic analysis of the formate synthesis from CO_2 and H_2 as well as the formate decomposition. However, no comparative kinetic study was performed concerning formate synthesis and decomposition between Cu powder catalysts and single-crystal surfaces under similar reaction conditions.

In this study, we focus on (i) the applicability of the Cu single-crystal surface to a Cu/SiO_2 powder catalyst as the model catalyst for the formate synthesis and the formate decomposition, (ii) the effect of SiO_2 upon their kinetics, and (iii) the promotional effect of H_2 upon the decomposition of formate seen for Cu(111).

2. EXPERIMENTAL

The 30 wt% Cu/SiO_2 catalyst was prepared by impregnation of Cab-O-Sil SiO_2 to incipient wetness with an aqueous solution of $Cu(NO_3)_2 \cdot 3H_2O$. The catalyst was dried at 393 K for 17 h and then calcined at 673 K for 2 h in air. Prior to the reactions, 1.0 g of catalyst was reduced with H_2 diluted with helium or N_2 to 10% (total pressure is 1 atm) at 523 K for 1–2 h in a flow reactor. The surface area of Cu for the reduced Cu/SiO_2 catalyst was measured to be 0.70 m^2 g-cat^{-1} by reaction with N_2O pulses (0.1–0.4 cc) at 363 K in a helium carrier gas, where the density of the surface copper atom was assumed to be 1.77×10^{15} atoms cm^{-2}.

The experiments were performed using a fixed-bed flow reactor connected to a gas chromatograph (GC). The synthesis of formate on the reduced Cu/SiO_2 catalyst was carried out by exposure to a reaction mixture of CO_2/H_2 (380 Torr/380 Torr, 1 Torr = 133.3 N m^{-2}) at 323–353 K with a flow rate of 40 cc min^{-1} for 2–120 min. Later, data will show that the decomposition of formate was negligible at these temperatures. After the formate synthesis, the catalyst was cooled to room temperature in an N_2 or helium stream to avoid the formate decomposition. In order to measure the coverage of formate, a temperature-programmed decomposition (TPD) experiment was carried out, in which the catalyst was heated to 523 K in the N_2 or helium stream with a heating rate of 2 K min^{-1} to decompose the formate into CO_2 and H_2. The decomposition products of CO_2 and H_2 were analyzed by GC using Molecular Sieve 5A and Porapak Q, respectively. The number of CO_2 and H_2 molecules was estimated from the TPD peak area using the relative sensitivity factors of CO_2 and H_2 (1:7.01) as well as an absolute calibration line for CO_2. When H_2 was present with CO_2 in the GC detector, the GC sensitivity of CO_2 decreased with increasing H_2 pressure. We calibrated the GC signal against the amount of CO_2. The formate coverage was then estimated from the surface area of Cu and the number of H_2 or CO_2 molecules.

The decomposition kinetics of formate was examined by an isothermal decomposition experiment at 384–417 K in the flow reactor. The formate was first synthesized in the reactor by exposing a reduced Cu/SiO_2 catalyst to a CO_2/H_2 (190 Torr/570 Torr) stream at 381 K with a flow rate of 40 cc/min. After the formate synthesis, the catalyst was cooled to room temperature in a helium stream. The catalyst was heated once to 353 K to desorb water impurities and then heated to a reaction temperature while the effluent CO_2 was successively analyzed by GC for a sufficient time.

The kinetic analysis of the isothermal formate decomposition was carried out in the way shown in Fig. 1, which shows a typical GC signal of the effluent CO_2 as a function of time (t). Here, A^{tot} and A correspond to the totally integrated peak area and the peak area integrated between t and the start of the preheating, respectively. Since the total coverage of formate (θ^{tot}_{HCOO}) can be calculated from the

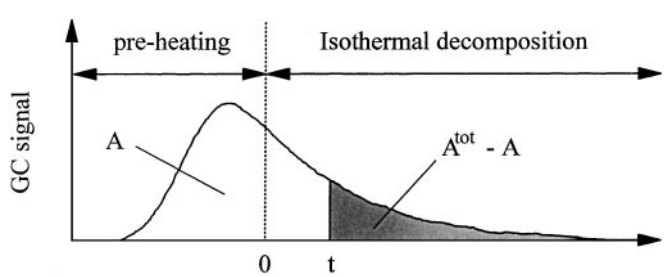

FIG. 1. GC signal of CO_2 formed by isothermal decomposition of formate on Cu/SiO_2 as a function of time.

surface area of Cu and the total peak area of desorbed CO_2, the formate coverage at t (θ_{HCOO}) during the isothermal experiment can be estimated by the following equation:

$$\theta_{HCOO} = [(A^{tot} - A)/A^{tot}]\theta^{tot}_{HCOO}. \quad [1]$$

The formate coverage (θ_{HCOO}) was thus determined by measuring A and A^{tot}. For low-temperature decomposition experiments, the catalyst was heated to high temperatures sufficient to decompose residual formate species in order to measure A^{tot}. In the experiments to examine the effect of H_2 upon the decomposition kinetics of formate, the formate on Cu/SiO_2 was decomposed in an H_2 stream diluted with helium. Also, at low temperatures and/or in the presence of H_2 the GC peak shown in Fig. 1 became small so that the coverage range analyzed was short because it was difficult to analyze the slope of the GC peak near the GC background.

Equilibrium formate coverage at 370–540 K was measured by the H_2 TPD experiment after the catalyst was cooled to room temperature. To minimize a change in formate coverage during the cooling, the reactor was cooled in the air using a drier (room temperature) after the heater was removed. The CO_2/H_2 reaction mixture was changed to the helium stream 10 s after the end of the reaction. The experimental error in the formate coverage due to the synthesis or the decomposition of formate during the cooling under the reaction mixture and helium was estimated on the basis of the kinetics of formate synthesis and formate decomposition as well as the cooling rate. We then set the error bar.

3. RESULTS AND DISCUSSION

3.1. Formate Synthesis

The formate synthesis by hydrogenation of CO_2 was carried out over a reduced Cu/SiO_2 catalyst at 323–353 K, at which the decomposition of formate was negligible. The amount of formate was determined by the GC peak area of CO_2 and H_2 formed by the decomposition of formate ($HCOO_a \rightarrow CO_2 + \frac{1}{2}H_2$) in the TPD experiments. Figure 2 shows typical TPD data for formate species synthesized from a CO_2/H_2 mixture of 190 Torr/570 Torr for 2 min at 381 K. The desorption peaks of CO_2 and H_2 were observed at 410 K, where the molar ratio of CO_2/H_2 was determined to be 2.34, in agreement with the stoichiometric value of 2. The desorption peak of TPD was comparable to the literature data of 400–473 K reported for Cu/SiO_2 (19), Cu(110) (21), Cu(100) (26), and Cu/ZnO(0001) (27), varying with the heating rate. Desorption of small amounts of H_2 was also detected around 330 K, which was attributed to residual hydrogen atoms on the Cu surface (28–30). The amount of hydrogen was constant regardless of the reaction time and the reaction temperature.

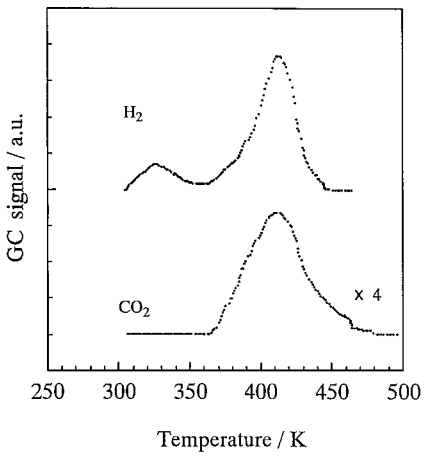

FIG. 2. TPD of formate on Cu/SiO_2. The formate species was synthesized from 190 Torr CO_2/570 Torr H_2 at 381 K.

Figure 3 shows the buildup curve of formate synthesized on Cu/SiO_2 from 380 Torr CO_2/380 Torr H_2 at 323–353 K for 2–120 min. While the TPD experiments were repeated, the coverage of formate at each reaction time was determined from the peak area of H_2 at 410 K and the Cu surface area. It was shown that the saturated formate coverage of 0.24 is in good agreement with that measured by XPS (11, 16) at the reaction temperature of 353 K using 380 Torr CO_2/380 Torr H_2. Furthermore, the saturated coverage agreed with that on Cu(111) obtained by the STM measurements (13), in which a $c(2 \times 4)$ structure corresponding to the coverage of 0.25 was observed for the formate synthesized from CO_2 and H_2 under the same reaction conditions as those in the XPS study. From the slope of the solid line at zero coverage in Fig. 3, we can derive the initial formation rate of formate at 323–353 K. The rates are shown as an Arrhenius plot in Fig. 4, where the reported data were indicated herein for

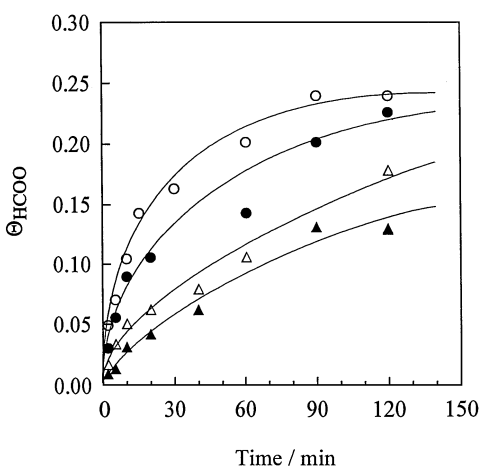

FIG. 3. Buildup of formate synthesized from 380 Torr CO_2/380 Torr H_2 at 323 K (▲), 333 K (△), 343 K (●), and 353 K (○).

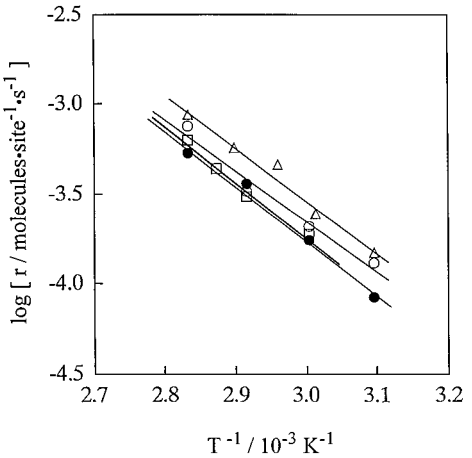

FIG. 4. Arrhenius plot of formate synthesis from 380 Torr CO_2/380 Torr H_2 on Cu/SiO_2 (●), with data for Cu(111) measured by XPS (11) (○) and IRAS (12) (△) and Cu(110) by IRAS (12) (□).

Cu(111) measured by XPS (11) and IRAS (12) as well as for Cu(110) measured by IRAS (12). As can be seen from Fig. 4, the absolute value of the initial rate on the Cu/SiO_2 powder catalyst in terms of molecules per site per second and the temperature dependence were in good agreement with those obtained for the Cu model catalysts. That is, the kinetics of the formate synthesis on the Cu/SiO_2 catalyst was basically the same as that for the copper single-crystal surfaces. As shown in Table 1, the apparent activation energy of the formate synthesis on Cu/SiO_2 (58.8 kJ mol^{-1}) obtained from the slope in Fig. 4 was comparable with those obtained for Cu(111), Cu(110), and Cu(100). It is also seen here that the formate synthesis on Cu is structure-insensitive, as previously reported (12).

3.2. Formate Decomposition

The decomposition kinetics of formate was measured at a constant temperature between 384 and 417 K in helium after preparation of the formate from a 190 Torr CO_2/570 Torr H_2 gas mixture at 381 K. The initial formate coverage was ~0.23. CO_2 and H_2 were the only products formed by the decomposition of formate. Assuming that the decomposition rate is first-order in formate coverage, the relationship between the rate constant and the formate coverage can be expressed by the following equations:

$$r_d = -d\theta_{HCOO}/dt = k_d\theta_{HCOO} \quad [2]$$

$$\int (1/\theta_{HCOO})\, d\theta_{HCOO} = -\int k_d\, dt \quad [3]$$

$$\log\theta_{HCOO} - \log\theta^0_{HCOO} = -k_d t. \quad [4]$$

Here, θ^0_{HCOO} is the formate coverage at $t = 0$. In the isothermal decomposition experiment, the rate constant was thus obtained by the slope of $\log(\theta_{HCOO}/\log\theta^0_{HCOO})$ vs t as shown in Fig. 5. The linear relationship seen in Fig. 5 clearly indicates that the decomposition rate of the formate is first-order in formate coverage, from which, for example, the rate constant was determined to be 1.13×10^{-4} s^{-1} at 384 K. The results of the first-order dependence have been reported for Cu(111) (12, 17), Cu(110) (12, 21), and Cu/SiO_2 (19) regardless of the preparation mode of formate, i.e., synthesis from CO_2 and H_2 or adsorption of formic acid, indicating that the formate species decomposes unimolecularly on Cu surfaces.

Figure 6 shows the Arrhenius plot of the rate constant for the formate decomposition on Cu/SiO_2 as well as Cu(111) (12, 17) and Cu(110) (12). The activation energy and the pre-exponential factor were derived from this figure as 115.7 kJ mol^{-1} and 5.38×10^{11} s^{-1}, respectively. In comparison, surface science data on copper single-crystal surfaces are given in Table 2, where a structure-sensitive character is seen for the formate decomposition on Cu. It is found here that the activation energy and the pre-exponential factor measured on Cu/SiO_2 are in good agreement with those obtained for Cu(111), 107.9–112.8 kJ mol^{-1} and (1.87–4.02) $\times 10^{11}$ s^{-1}, rather than Cu(110) and Cu(100); thus, the surface of Cu particles in Cu/SiO_2 is expected to comprise

TABLE 1

Apparent Activation Energy and Pre-exponential Factor for Formate Synthesis

Catalyst	Method	E_a/kJ mol^{-1}	Ref.
Cu/SiO_2	GC	58.8	This work
Cu(111)	XPS	54.6	11
Cu(111)	IRAS	56.6	12
Cu(110)	IRAS	59.8	12
Cu(100)	XPS	55.6	26

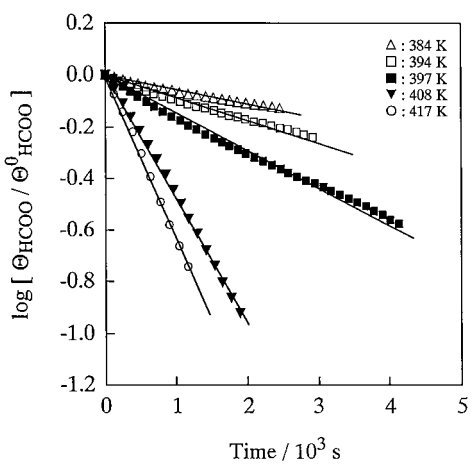

FIG. 5. $\log(\theta_{HCOO}/\theta^0_{HCOO})$ vs reaction time during the isothermal decomposition of formate on Cu/SiO_2.

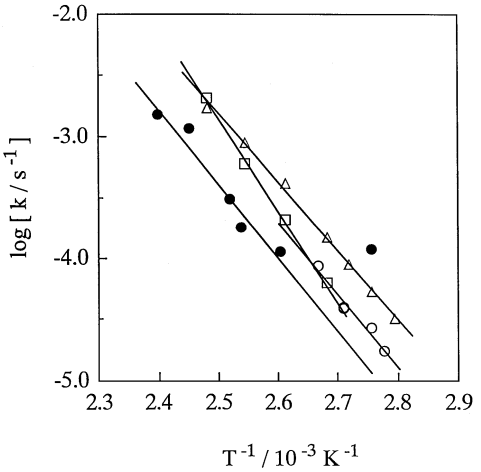

FIG. 6. Arrhenius plot of the rate constant for the formate decomposition on Cu/SiO_2 (●) with data for Cu(111) measured by XPS (17) (○) and IRAS (12) (△) and Cu(110) by IRAS (12) (□).

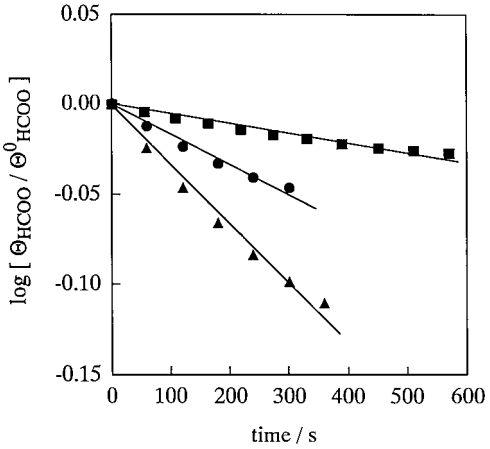

FIG. 7. $\log(\theta_{HCOO}/\theta^0_{HCOO})$ vs reaction time during the isothermal decomposition of formate on Cu/SiO_2 at 363 K in the presence of H_2. $P_{H_2} = 0$ (■), 303 (●), and 457 (▲) Torr diluted with helium.

the most densely packed Cu(111) plane. Considering the results of Section 3.1, that is, the kinetics of formate synthesis, the Cu(111) surface can be regarded as a model of the Cu/SiO_2 powder catalyst prepared in this study. Interestingly, the decomposition of the formate on Cu is structure-sensitive, although the formation of formate is structure-insensitive as described in Section 3.1. The detailed surface chemistry will be published elsewhere (18).

3.3. Formate Decomposition in H_2

We have incidentally found that the rate of the formate decomposition on Cu(111) is accelerated by the presence of H_2. Interestingly, the promotion was observed for Cu(111), but not for Cu(110) (18). We thus examined the promotion in the formate decomposition on the Cu/SiO_2 powder catalyst. The decomposition rate of formate synthesized from a CO_2/H_2 mixture of 190 Torr/570 Torr was measured on Cu/SiO_2 in H_2 diluted with helium. Figure 7 shows representative results of the isothermal decomposition experiments at 363 K in pure helium, 303 Torr H_2, and 457 Torr H_2. As described in Section 3.2, the slope of $\log(\theta_{HCOO}/\log\theta^0_{HCOO})$ vs t gives the decomposition rate constant. It is clearly demonstrated that the presence of H_2 promotes the decomposition of formate by a factor of 6 at the H_2 pressure of 457 Torr. The linearity shown in Fig. 7 indicates that formate decomposes unimolecularly even in the presence of H_2. The dependence of H_2 pressure on the decomposition rate was examined by varying the H_2 pressure while keeping the reaction temperature at 363 K. Figure 8 shows the initial decomposition rate of formate at $\theta_{HCOO} = 0.24$ as a function of the H_2 pressure on Cu/SiO_2 with data obtained for Cu(111) (18). As shown in Fig. 8, the promotion curve measured for Cu/SiO_2 was very similar to that obtained for Cu(111), supporting that the Cu(111) surface is the model for Cu/SiO_2. We checked that the promotion by H_2 was not due to the consumption of formate by hydrogenation into formic acid. That is, no formic acid nor

TABLE 2

Activation Energy and Pre-exponential Factor for Decomposition of Formate Synthesized by Hydrogenation of CO_2

Catalyst	Method	E_a/kJ mol^{-1}	ν/s^{-1}	Ref.
Cu/SiO_2	GC	115.7	5.38×10^{11}	This work
Cu(111)	XPS	112.8	4.02×10^{11}	17
Cu(111)	IRAS	107.9	1.87×10^{11}	12
Cu(110)	IRAS	145.2	1.22×10^{16}	12
Cu(100)	TPD	130–155[a]		26

[a] From the energy diagram in Ref. (26).

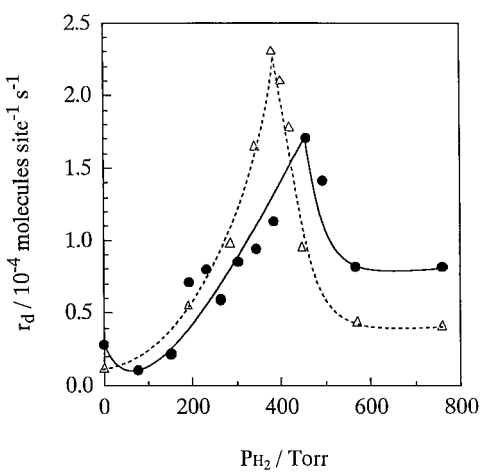

FIG. 8. Effect of H_2 on the initial rate of formate decomposition on Cu/SiO_2 (●) at 363 K in comparison with data for Cu(111) (△).

the decomposition product of CO_2 was detected upon introduction of 456 Torr H_2 over the formate-adsorbed Cu/SiO_2 catalyst. The peak for Cu/SiO_2 was shifted to higher pressure compared to those of Cu(111) and Cu(111) as shown in Fig. 8, which was thought to be an effect of SiO_2 as discussed in Section 3.4.

The promotional effect of H_2 upon the decomposition rate can be related to the adsorption structure of the formate on Cu. First, a very characteristic relationship has been observed between the decomposition kinetics and the structure of formate on Cu(111). That is, the formate species prepared by adsorption of formic acid in UHV decomposed faster by a factor of 17 than the formate synthesized from CO_2 and H_2, and the adsorption structures of formate on Cu(111) were different depending on the preparation method. As for the synthesis from CO_2 and H_2, chains consisting of formate molecules were observed at low formate coverage with the distance between the formate molecule being twice the nearest-neighbor distance of Cu atoms. With increasing formate coverage, the distance between the chains was reduced to form various ordered structures, indicating that the formate–formate interaction in a chain is attractive, whereas the interaction between the chains is repulsive. However, no chain structure was observed for the formate prepared by adsorption of formic acid. At the low formate coverage, no single formate species can be imaged by STM at room temperature, indicating that formate diffuses on Cu(111) more rapidly than the scanning of the STM tip. With increasing formate coverage, $p(4 \times 4)$ and then $(3 \times \frac{7}{2})$ structures appeared, but no chain structure was observed at any formate coverage. Accordingly, the difference seen in the decomposition kinetics of formate depending on the preparation method was in their adsorption structure. Most interestingly, the decomposition rates of the synthesized formate in the presence of H_2 at the maxima were exactly the same as those of the formate prepared from formic acid. Probably, the chain structure of the synthesized formate will collapse in the presence of H_a by an interaction between H_a and formate, leading to an increase in the decomposition rate of formate.

We briefly discuss the relationship between the decomposition kinetics and the adsorption structure (13). Although the decomposition rate of the formate prepared from formic acid was greater than that of the formate prepared from CO_2 and H_2, the activation energy was identical. The difference in the decomposition rate is thus due to changes in the pre-exponential factor of the rate constant, or the frequency factor in the transition state of the decomposition. The transition state of the formate decomposition may be passed by the OCO vibration toward the surface, which determines the frequency factor. In the chain structures, the OCO plane vibration will be inhibited by the nearest-neighbor formate species, leading to a decrease in the frequency factor.

We also thought that at higher H_2 pressures above 500 Torr in Fig. 8 the high coverage of H_a blocked the Cu site required for the transition state of the decomposition, leading to a decrease in the decomposition rate of formate.

3.4. *Equilibrium Coverage and Effect of SiO_2*

Equilibrium formate coverage on Cu/SiO_2 during the hydrogenation of CO_2 was measured using the TPD experiment, which was then compared with that calculated from the kinetics of the formate synthesis and the formate decomposition described in Sections 3.1–3.3. The hydrogenation of CO_2 was carried out at 353–539 K for 90–120 min using a mixture of 380 Torr CO_2 and 380 Torr H_2. The measured formate coverage is shown by closed circles in Fig. 9 as a function of reaction temperature. The calculated formate coverage is also shown here as a solid line based on the following equations:

$$r_f = r_{f0}\{1 - (\theta_{HCOO}/0.24)\} \quad [5]$$

$$r_d = k'_d\theta_{HCOO} \quad [6]$$

$$\theta_{HCOO} = r_{f0}/\{(r_{f0}/0.24) + k'_d\}. \quad [7]$$

Here, it is assumed that the initial formation rate of the formate (r_{f0}) is first-order in formate coverage, and the saturated formate coverage is 0.24. k'_d is the rate constant for the decomposition of formate in the presence of 380 Torr H_2. The k'_d was calculated from the rate constant at 363 K and 380 Torr H_2 in Fig. 8 as well as the activation energy (115.7 kJ mol^{-1}) of the formate decomposition on Cu/SiO_2 in the absence of H_2, based on the fact that the activation energy was identical, independent of the H_2 pressure on Cu(111) (18). It is clearly shown that the measured formate coverage can be well reproduced by the calculated

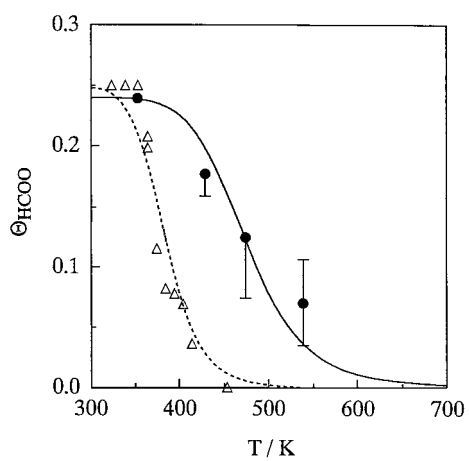

FIG. 9. Equilibrium formate coverage under the hydrogenation of CO_2 at 380 Torr CO_2/380 Torr H_2 on Cu/SiO_2 (●) in comparison with data for Cu(111) (△). The solid curves are the calculated coverage based on the kinetic model and the points are the measured coverage.

coverage based on the kinetics of Eqs. [5] and [6] measured separately; thus, the kinetics reported in this study is applicable to estimate the surface formate coverage on the Cu/SiO_2 catalyst under the steady state of the CO_2 hydrogenation at any reaction temperature.

In comparison, the results of Cu(111) are also shown in Fig. 9 (18). The reaction conditions are exactly the same as those for Cu/SiO_2. Similarly to Cu/SiO_2, the measured formate coverage in equilibrium is in good agreement with that calculated from the kinetics of the formate synthesis and the formate decomposition. However, the formate coverage on Cu(111) was less than that on Cu/SiO_2. This can be ascribed to the difference shown in Fig. 8; that is, the decomposition rate on Cu/SiO_2 at 380 Torr H_2 is lower than that on Cu(111), leading to the relatively large equilibrium formate coverage on Cu/SiO_2. In other words, the difference lies in the peak shift of the decomposition rate on Cu/SiO_2 to higher H_2 pressures compared to that for Cu(111). This was the only effect of SiO_2 observed in the chemistry of formate on the Cu/SiO_2 catalyst.

We have argued here that the surface of Cu particles supported on SiO_2 comprises Cu(111) planes because between Cu/SiO_2 and Cu(111) (i) the kinetics of the formate synthesis is identical (Section 3.1), (ii) the kinetics of the formate decomposition in UHV is identical (Section 3.2), and (iii) the promotional effect of H_2 on the decomposition rate is observed, but is not observed for Cu(110) (Section 3.3). Although these kinetics are basically identical between Cu/SiO_2 and Cu(111), the effect of SiO_2 was seen in the hydrogen-promoting decomposition kinetics on Cu (Fig. 8) . We currently consider that atomic hydrogen coverage on Cu determining the decomposition rate may be decreased by the presence of SiO_2. That is, atomic hydrogen formed by dissociation of H_2 on Cu spills over onto the surface of the SiO_2 support, leading to the decrease in the hydrogen coverage on Cu. The mechanism of the hydrogen promotion, its structure sensitivity, and the spillover model are still under investigation.

4. CONCLUSIONS

(1) The kinetics of formate synthesis from CO_2 and H_2 and from formate decomposition were measured on a Cu/SiO_2 catalyst, which basically agreed with those reported for Cu(111) in terms of the activation energy, the order of the reactions, and the absolute reaction rate. This indicates that the Cu(111) surface can be regarded as a model catalyst for Cu/SiO_2 catalysts.

(2) The promotional effect of H_2 upon decomposition of the formate was observed on the Cu/SiO_2 catalyst as previously observed for Cu(111) but not for Cu(110); this again supports that the surface of Cu particles in the Cu/SiO_2 catalyst comprises Cu(111) planes.

(3) The measured equilibrium formate coverage during the hydrogenation of CO_2 at 353–539 K was in good agreement with that calculated from the kinetics of the formate synthesis and the formate decomposition measured separately, where the promotional effect of H_2 on the decomposition is considered. However, the equilibrium coverage on Cu/SiO_2 was greater than those measured and calculated for Cu(111). This is explained by an effect of SiO_2 upon hydrogen coverage on the Cu surface, where hydrogen atoms formed by dissociation of H_2 on Cu spill over onto the SiO_2 surface, leading to a decrease in hydrogen coverage on Cu.

REFERENCES

1. Campbell, C. T., *Adv. Catal.* **36**, 1 (1989).
2. Rodriguez, J. A., and Goodman, D. W., *Surf. Sci. Rep.* **14**, 1 (1991).
3. Fujitani, T., Saito, M., Kanai, Y., Kakumoto, T., Watanabe, T., Nakamura, J., and Uchijima, T., *Catal. Lett.* **25**, 271 (1994).
4. Kanai, Y., Watanabe, T., Fujitani, T., Saito, M., Nakamura, J., and Uchijima, T., *Catal. Lett.* **27**, 67 (1994).
5. Kanai, Y., Watanabe, T., Fujitani, T., Uchijima, T., and Nakamura, J., *Catal. Lett.* **38**, 157 (1996).
6. Fujitani, T., Matsuda, T., Kushida, Y., Ogihara, S., Uchijima, T., and Nakamura, J., *Catal. Lett.* **49**, 175 (1997).
7. Fujitani, T., and Nakamura, J., *Catal. Lett.* **56**, 119 (1998).
8. Fujitani, T., Nakamura, I., Uchijima, T., and Nakamura, J., *Surf. Sci.* **383**, 285 (1997).
9. Nakamura, I., Fujitani, T., Uchijima, T., and Nakamura, J., *Surf. Sci.* **400**, 387 (1998).
10. Nakamura, I., Nakano, H., Fujitani, T., Uchijima, T., and Nakamura, J., *Surf. Sci.* **402–404**, 92 (1998).
11. Nakamura, J., Kushida, Y., Choi, Y., Uchijima, T., and Fujitani, T., *J. Vac. Sci. Technol. A* **15**, 1568 (1997).
12. Nakamura, I., Nakano, H., Fujitani, T., Uchijima, T., and Nakamura, J., *J. Vac. Sci. Technol. A* **17**, 1592 (1999).
13. Fujitani, T., Choi, Y., Sano, M., Kushida, Y., and Nakamura, J., *J. Phys. Chem.* **104**, 1235 (2000).
14. Morikawa, Y., Iwata, K., Nakamura, J., Fujitani, T., and Terakura, K., *Chem. Phys. Lett.* **304**, 91 (1999).
15. Fujitani, T., and Nakamura, J., *Appl. Catal. A* **191**, 111 (2000).
16. Fujitani, T., Nakamura, I., Ueno, S., Uchijima, T., and Nakamura, J., *Appl. Surf. Sci.* **121/122**, 583 (1997).
17. Nishimura, H., Yatsu, T., Fujitani, T., Uchijima, T., and Nakamura, J., *J. Mol. Catal.*, in press.
18. Nakano, H., Nakamura, I., Fujitani, T., and Nakamura, J., in preparation.
19. Iglesia, E., and Boudart, M., *J. Phys. Chem.* **90**, 5272 (1986).
20. Iglesia, E., and Boudart, M., *J. Catal.* **81**, 214 (1983).
21. Ying, D. H. S., and Madix, R. J., *J. Catal.* **61**, 48 (1980).
22. Bowker, M., and Madix, R. J., *Surf. Sci.* **102**, 542 (1981).
23. Hayden, B. E., Prince, K., Woodruff, D. P., and Bradshaw, A. M., *Surf. Sci.* **133**, 589 (1983).
24. Dubois, L. H., Ellis, T. H., Zegarski, B. R., and Kevan, S. D., *Surf. Sci.* **172**, 385 (1986).
25. Sexton, B. A., *Surf. Sci.* **88**, 319 (1979).
26. Taylor, P. A., Rasmussen, P. B., Ovesen, C. V., Stoltze, P., and Chorkendorff, I., *Surf. Sci.* **261**, 191 (1992).
27. Yoshihara, J., and Campbell, C. T., *Surf. Sci.* **407**, 256 (1998).
28. Sandoval, M. J., and Bell, A. T., *J. Catal.* **144**, 227 (1993).
29. Anger, G., Winkler, A., and Rendulic, K. D., *Surf. Sci.* **220**, 1 (1989).
30. Tabatabaei, J., Sakakini, B. H., Watson, M. J., and Waugh, K. C., *Catal. Lett.* **59**, 151 (1999).